


RESEARCH ARTICLE

Individual differences in decision making competence revealed by multivariate fMRI

Tanveer Talukdar^{1,2}  | Francisco J. Román^{1,2} | Joachim T. Operskalski^{1,2} | Christopher E. Zwilling^{1,2} | Aron K. Barbey^{1,2,3,4,5,6}

¹Decision Neuroscience Laboratory, University of Illinois, Urbana, Illinois

²Beckman Institute for Advanced Science and Technology, University of Illinois, Urbana, Illinois

³Department of Psychology, University of Illinois, Urbana, Illinois

⁴Department of Internal Medicine, University of Illinois, Champaign, Illinois

⁵Department of Bioengineering, University of Illinois, Champaign, Illinois

⁶Carle R. Woese Institute for Genomic Biology, University of Illinois, Champaign, Illinois

Correspondence

Tanveer Talukdar and Aron K. Barbey, Decision Neuroscience Laboratory, Beckman Institute for Advanced Science and Technology, University of Illinois at Urbana-Champaign, 405 North Mathews Avenue, Urbana, IL 61801, USA. Emails: ttanveer@illinois.edu; barbey@illinois.edu

Funding information

Office of the Director of National Intelligence (ODNI), Intelligence Advanced Research Projects Activity (IARPA), Grant/Award Number: 2014-13121700004

Abstract

While an extensive literature in decision neuroscience has elucidated the neurobiological foundations of decision making, prior research has focused primarily on group-level effects in a sample population. Due to the presence of inherent differences between individuals' cognitive abilities, it is also important to examine the neural correlates of decision making that explain interindividual variability in cognitive performance. This study therefore investigated how individual differences in decision making competence, as measured by the Adult Decision Making Competence (A-DMC) battery, are related to functional brain connectivity patterns derived from resting-state fMRI data in a sample of 304 healthy participants. We examined connectome-wide associations, identifying regions within frontal, parietal, temporal, and occipital cortex that demonstrated significant associations with decision making competence. We then assessed whether the functional interactions between brain regions sensitive to decision making competence and seven intrinsic connectivity networks (ICNs) were predictive of specific facets of decision making assessed by subtests of the A-DMC battery. Our findings suggest that individual differences in specific facets of decision making competence are mediated by ICNs that support executive, social, and perceptual processes, and motivate an integrative framework for understanding the neural basis of individual differences in decision making competence.

KEYWORDS

Adult Decision Making Competence (A-DMC), individual difference, multivariate analysis, resting-state fMRI

1 | INTRODUCTION

Decision making is ubiquitous in daily life and depends on forming preferences, selecting and executing actions, and evaluating outcomes. Recent decades have seen remarkable progress in understanding the behavioral, cognitive, and neural processes that underlie decision making. Research to elucidate its neurobiological foundations would not only advance our understanding of the nature of human decision making, but would also facilitate clinical research that targets the underlying neural mechanisms in an effort to facilitate decision making in psychiatric illness and neurological disease. Emerging evidence from neuroimaging studies indicates that multiple brain regions and networks are associated with specific facets of decision making. For example, value-

based decision making has been shown to engage the ventromedial and dorsolateral prefrontal cortex (Rudolf & Hare, 2014); decisions based on probabilistic reasoning have been associated with activity in the parietal cortex (Kiani & Shadlen, 2009; Shadlen & Newsome, 2001; Yang & Shadlen, 2007); while decision making under risk or uncertainty has been associated with activity in the orbitofrontal cortex, medial prefrontal cortex, caudate, and rostral anterior cingulate cortex (Krain, Wilson, Arbuckle, Castellanos, & Milham, 2006). In addition, reward-based decision making is known to engage the limbic system, comprising regions such as the amygdala, insula cortex, and basal ganglia (Lee, 2008; Marschner, et al., 2005).

Further evidence to elucidate the neurobiological properties of decision making is provided by lesion-symptom mapping studies

(Bechara, Tranel, & Damasio, 2000b; Fellows & Farah, 2004; Glascher, et al., 2012; Stuss, et al., 2000). In particular, the work by Glascher et al., 2012, represents one of the largest lesion-based studies to examine reward-based decision making—demonstrating that the ventral prefrontal cortex plays a central role. The capacity to represent somatic states (e.g., feelings and emotions) that guide reward-based decision making are also known to engage the orbitofrontal cortex (Bechara, Damasio, & Damasio, 2000a; Hornak, et al., 2003).

Despite remarkable advances in understanding the neurobiological mechanisms of human decision making, several well-known challenges remain. Often, experimental paradigms designed to measure decision making competence do not reflect real world choices. Importantly, humans exhibit sizeable interindividual differences in decision making—revealed through the application of neuropsychological tests that are designed to capture heterogeneity and by applying computational approaches that can model individual differences. The widely established role of individual differences in decision making in cognitive psychology prompted us to explore the underlying neural correlates of individuals' decision making abilities based on the Adult Decision Making Competence (A-DMC) test. (Bruine de Bruin, Parker, & Fischhoff, 2007). The A-DMC battery has been shown to reliably predict individual differences in decision making competence and is associated with a wide range of real-world decisions—spanning social, economic, and medical decision making. The A-DMC provides a comprehensive assessment of core facets of decision making, including consistency in risk perception (ability to perform probabilistic reasoning), resistance to framing (understanding positive or negative valence effects), resistance to sunken costs (ability to ignore prior belief in decision outcomes), applying decision rules (weighing decision options), social norms (ability to accurately judge the normative beliefs of one's peers), and over/under confidence (extent of self-awareness).

Using a data-driven approach, we investigated whether individual differences in decision making competence (as measured from the A-DMC) are related to interindividual variability in resting-state functional connectivity across the entire brain connectome. Applying multivariate distance-based matrix regression (MDMR) (Shehzad, et al., 2014; Talukdar et al., 2017), we first identified brain regions sensitive to composite A-DMC scores comprised of individuals' responses on six subtests measuring specific facets of decision making. We then applied structural equation modeling (SEM) to investigate whether A-DMC sensitive regions and their degree of influence on seven intrinsic connectivity networks (ICNs) (Yeo, et al., 2011) were predictive of individual subtests of decision making competence. The seven ICNs under investigation included the fronto-parietal network, dorsal attention network, ventral attention network, default mode network, limbic network, visual network, and somatomotor network (Laird, et al., 2011). Using path analysis, we explored the direction and magnitude of association between the observed neurobiological markers and individual differences in decision making competence.

This study therefore sought to elucidate (1) how decision making competence is shaped by individual differences in the functional brain connectome and (2) how the functional connectivity of the observed brain regions—and their capacity to influence core ICNs—underlies

specific facets of decision making competence. Our approach takes advantage of a multivariate analysis framework that is designed to map contributions from multiple sets of functional connections across the entire brain to explain individual differences in decision making competence. A multivariate approach enables an assessment of the functional brain connectome—examining distributed patterns of brain activity in their entirety—and therefore represents a methodological advance over standard univariate methods. A multivariate approach also provides a novel lens for examining individual differences, which standard group-level statistics are unable to address. Furthermore, our application of the SEM framework allows an investigation of the effects of network influence on specific facets of decision making competence, providing an opportunity to elucidate how decision making processes are shaped by individual differences in the functional brain connectome.

2 | METHODS

2.1 | Participants

Three hundred and four participants were enrolled in the study (male: 147, female: 157, ages 18–43 years, mean 23.3 ± 5.1 years). All participants were clinically healthy, native English speakers with normal or corrected-to-normal vision. Each participant provided written informed consent in accordance with guidelines established by the University of Illinois Institutional Review Board for resting-state fMRI scans and administration of the A-DMC battery.

2.2 | MRI data acquisition

All data were collected on a Siemens Magnetom 3T Trio scanner using a 32-channel head coil in the MRI Laboratory of the Beckman Institute Biomedical Imaging Center at the University of Illinois.

A high-resolution multi-echo T1-weighted magnetization prepared gradient-echo structural image was acquired for each participant (0.9 mm isotropic, TR: 1,900 ms, TI: 900 ms, TE = 2.32 ms, with GRAPPA and an acceleration factor of 2). The functional neuroimaging data were acquired using an accelerated gradient-echo echoplanar imaging (EPI) sequence (Auerbach, Xu, Yacoub, Moeller, & Uğurbil, 2013), sensitive to blood oxygenation level dependent (BOLD) contrast ($1.9 \times 1.9 \times 2.0$ mm voxel size, 56 slices with 10% slice gap, TR = 2,000 ms, TE = 30 ms, FOV = 240 mm, 90° flip angle, 10 min acquisition, or 300 volumes). During the resting-state fMRI scan, participants were shown a white crosshair on a black background viewed on an LCD monitor through a head coil-mounted mirror. Participants were instructed to lie still, focus on the visually presented cross hair, and to keep their eyes open (Van Dijk, et al., 2010).

2.3 | MRI preprocessing

All MRI data processing was performed using FSL tools available in FMRIB Software Library version 5.0 (<http://fsl.fmrib.ox.ac.uk/fsl/fslwiki/>). The high-resolution T1 MPRAGE was brain extracted using the BET analysis tool (Smith, 2002). FAST segmentation (Zhang, Brady, & Smith, 2001) was performed to delineate gray matter, white matter,

and CSF voxels. The resting-state fMRI data were preprocessed using the FSL FEAT analysis tool (Jenkinson, Beckmann, Behrens, Woolrich, & Smith, 2012; Satterthwaite, et al., 2013). Preprocessing entailed: slice timing correction, motion correction, spatial smoothing (3 mm FWHM kernel), nuisance signal regression (described below), temporal band-pass filtering (0.009–0.1 Hz), linear registration of functional images to structural images, and nonlinear registration of structural images to the MNI152 brain template (2 mm isotropic voxel resolution).

Nuisance variables were modeled via GLM analyses to remove spurious correlations, noise introduced by head motion, in addition to variables of no interest such as signal changes in the white matter and the cerebrospinal fluid. The set of nuisance regressors in the GLM analysis therefore included head motion correction parameters (using the extended 12 motion parameters estimated in the FEAT preprocessing), individual volume motion outliers estimated using DVARS (Power, Barnes, Snyder, Schlaggar, & Petersen, 2012) (outliers flagged using the boxplot cutoff $1.5 \times \text{IQR}$), and mean white matter and cerebrospinal fluid signals averaged across all voxels identified from the segmentation of the high-resolution MPRAGE. The fully preprocessed resting-state fMRI data were taken as the residuals from this GLM model. The residuals were transformed into normalized MNI152 space and resampled to 4 mm isotropic voxels.

2.4 | Adult Decision Making Competence (A-DMC) battery

The A-DMC measures fundamental competencies of decision making (Bruine de Bruin, et al., 2007). Six of the seven original subtests from the A-DMC battery were included in this study (i.e., the path independence subtest was excluded due to its low retest reliability) (Bruine de Bruin, et al., 2007). A description of each A-DMC subtest and associated dependent measure is summarized below.

2.4.1 | Consistency in risk perception

This test examines whether the respondent evaluates risk in an internally consistent manner (Bruine de Bruin, et al., 2007). For example, the respondent is asked to assess the likelihood of complementary events in which the probability of the subset (e.g., “dying in a terrorist attack”) should not exceed that of the superset (e.g., “dying from any cause”) to satisfy the criterion of internal consistency. Respondents are scored on the basis of correctly identifying the likelihood of those events based on probabilistic rules in set theory.

2.4.2 | Recognizing social norms

This test measures how well the respondents can accurately estimate social norms based on the beliefs of their peer group (Jacobs, Greenwald, & Osgood, 1995). The respondent is asked to judge whether undesirable behaviors (e.g., “to steal”) are socially acceptable and then is asked to estimate how many “out of 100 people your age” would endorse each behavior. Performance on this task is measured by the rank-order correlation between the observed and estimated percentage of peer endorsements.

2.4.3 | Resistance to sunken costs

This test measures the extent to which an individual ignores prior investments (i.e., sunken costs) and focuses instead on outcomes of their actions when making a decision (Arkes & Blumer, 1985). Responses are scored on a 6-point Likert scale, where the lowest point “1” indicates preference for the sunken-cost option, whereas the highest point “6” implies preference for the normatively correct option, which reflects the ability to ignore the past losses and focus only on future gains. The overall resistance to sunken costs score is determined by averaging the responses across all items in this subtest.

2.4.4 | Resistance to framing

This test measures the extent to which framing equivalent choices as gains or losses can influence the respondent’s preference (Tversky & Kahneman, 1981). The respondent is presented a pair of questions that differ only in the way that they are framed—either positively (gains) or negatively (loss). For instance, in a hypothetical case in which 1,200 endangered animals are threatened by a pesticide, a positive framing of the question would ask the participant to choose between two alternative forms of responses—they could *save* 600 animals or they can choose the alternative that results in a 75% chance that 800 animals will be *saved* and a 25% chance that 0 animals will be *saved*. The negative frame maintains the same wording, except the italicized words *save/saved* are replaced with *lose/lost*, along with the complementary numbers being presented to maintain statistical equivalence (e.g., a 75% chance that 800 animals will be saved is the same as a 75% chance that 400 animals will be lost). Responses are scored on a 6-point Likert scale. The resistance to framing score represents the mean of the absolute values of the differences between each pair of items, for all item pairs.

2.4.5 | Applying decision rules

This test measures the respondent’s ability to apply a specific set of decision rules when making a choice (i.e., elimination by key features, satisficing, lexicographic order, or equal weights; Payne, Bettman, & Johnson, 1993). This test provides a set of priorities for a customer and a set of product options under consideration by the customer. Respondents select one answer from a set of multiple-choice options and the number of correct responses determines the overall score.

2.4.6 | Under/over confidence

This test measures the extent to which a person recognizes the limits of their knowledge (Bruine de Bruin, et al., 2007). The respondent is first asked to provide a binary (true/false) response to a question requiring general knowledge about the world. The respondent then is asked to rate the degree of confidence they have in their response—applying a scale from 50% (just guessing) to 100% (absolutely sure). The overall under/over confidence score is then determined by subtracting from 1 the absolute value of the difference between the mean confidence rating and percentage correct across all items.

Results from the six A-DMC subtests were averaged to generate a composite score for each respondent, which provided an index of decision making competence for further investigation within MDMR.

2.5 | Multivariate distance-based matrix regression (MDMR)

MDMR was used to investigate whether individual differences in decision making competency (as measured by participants' A-DMC composite scores) are associated with resting-state functional connectivity. The MDMR analysis pipeline involves (1) extracting resting-state preprocessed BOLD time series signal from participants' fMRI scans; (2) computing a distance matrix indicating pairwise dissimilarity between participants' functional connectivity profiles for each brain region; (3) performing multivariate regression using the A-DMC composite scores as inputs and the distance matrix computed for each brain region as output; and (4) generating a statistical map of brain regions, which have significant associations with individuals' A-DMC composite scores. MATLAB R2014a was used to generate code and analysis scripts for performing the MDMR analysis. Craddock's 800 parcellated brain atlas in MNI space (Craddock et al., 2012) was applied as a mask to extract the mean BOLD time course from grey matter voxels within each parcel. A large parcellation consisting of 800 grey matter units was chosen to maintain regional specificity and also because test analysis by Shehzad et al. (2014) revealed substantial overlap at this resolution with whole-brain, voxel-wise MDMR analyses.

The distance matrix used in MDMR was derived from individual differences in functional connectivity profiles between each brain parcel. For each participant, functional connectivity was computed from pairwise correlations between mean BOLD time courses extracted from grey matter parcels that were common to all participants. A total of 662 parcellated regions (out of the 800 parcels) were found to be common across all participants. The correlations were Fisher's Z -transformed to improve normality. Next, dissimilarities between participants' functional connectivity profiles were calculated based on the distance metric $d = \sqrt{2(1-r)}$, where r represents the Pearson correlation between the connectivity profiles for a participant pair and brain region. All pairwise dissimilarities were then entered into a distance matrix. MDMR was then applied in the final step to test the degree to which the composite A-DMC scores explained variability in the distances between participants' functional connectivity profiles at each region separately.

The statistical parametric map computed from the MDMR analysis is a pseudo- F statistic, which represents the proportion of variance in distances accounted for by the individual differences in A-DMC composite scores. As the pseudo- F statistic does not have a known null distribution, significance was determined by permutation testing. A null distribution was simulated by performing 10,000 random permutations of the participant indices and computing the pseudo- F statistic at each iteration. A p value was then computed for each region by comparing the pseudo- F statistic from the original data to the simulated null distribution. The p values were converted to one-sided Z -scores and adjusted for multiple comparisons using Gaussian Random Field (GRF) correction (Li, Guo, Nie, Li, & Liu, 2009). GRF correction was performed using Matlab based toolbox for Data Processing & Analysis of Brain Imaging (DPABI) found at

<http://rfmri.org/DPABI>. The Z -scores were then projected back onto the MNI152 brain template. Next, FSL "autoaq" tool was used to determine center of mass (COM) coordinates of clustered regions by applying a voxel level threshold of $Z > 2.3$ ($p < .01$) and a minimum cluster size of 10 voxels.

2.6 | Structural equation modeling (SEM)

The SEM framework was implemented to investigate associations between A-DMC scores on the six subtests and measures of network influence of A-DMC sensitive regions functionally linked to each ICN. The A-DMC subtest scores obtained for all participants were adjusted for age and gender. Measures of network influence of A-DMC sensitive regions were derived from connectivity strength, which represents the sum of all neighboring connection weights/links for a given brain region/node (Rubinov & Sporns, 2010). A brief description of this analysis is presented below.

2.6.1 | Connectivity strength metric

Using a graph theoretical approach, nodes were defined as center of mass coordinates of the Craddock's parcellation units and edges as the standard normal Z -score of the Fisher's Z transformed correlation values between pairs of nodes for each subject. To transform Fisher's Z into standard normal Z -scores, the Fisher's Z were multiplied by their standard deviation approximated as $\sigma = 1/\sqrt{(n-3)}$, where n is the number of samples comprising the BOLD signal. The edges were next Bonferroni-corrected by applying a statistical Z -threshold to identify significant positive correlations ($p < .05$) (Fox, Zhang, Snyder, & Raichle, 2009; Murphy, Birn, Handwerker, Jones, & Bandettini, 2009). The thresholded Z -scores were then rescaled to represent connection weights ranging from 0 to 1. Based on these positive connection weights, subject-wise weighted connectivity matrices were generated, which represented functional connectivity between nodes corresponding to A-DMC sensitive regions (MDMR nodes) and those identified for each of the ICNs were generated (grey matter mask representative of the ICNs is available for download at https://surfer.nmr.mgh.harvard.edu/fswiki/Cortical-Parcellation_Yeo2011). Next, measures of total connectivity strength were computed as the sum of the connection weights of MDMR nodes linked to each ICN normalized by their node density. Measures of network influence were eventually derived from the average total connectivity strength of all MDMR nodes across each ICN.

2.6.2 | SEM path analysis model

The software Mplus (Muthén & Muthén, 2007) was used to explore the effects of the A-DMC sensitive regions' network influence on each ICN with respect to the individual A-DMC subtests. The directed dependencies of measures of network influence with respect to each ICN on every subtest of the A-DMC battery were evaluated. In addition, the covariations between measures of network influence and the covariations between each of the subtests were estimated.

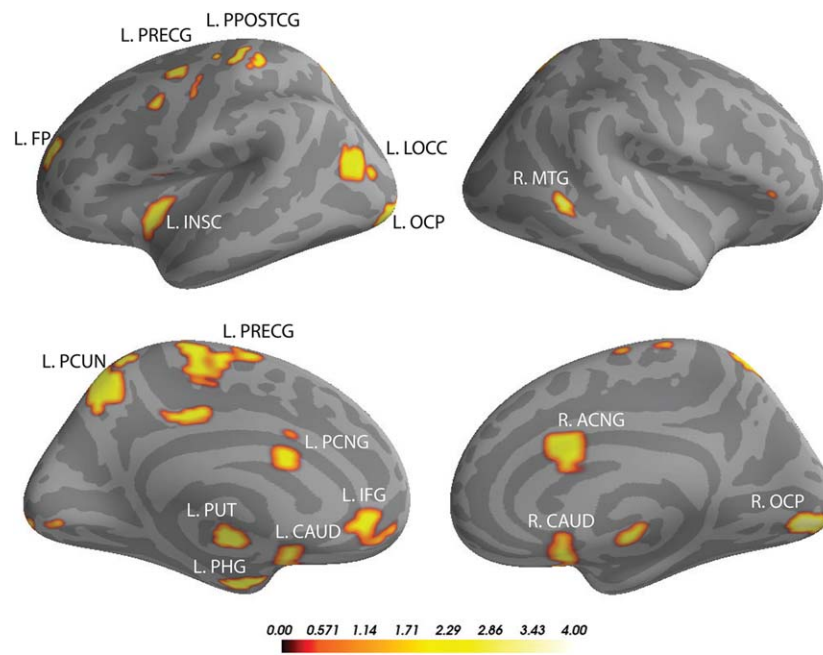


FIGURE 1 Multivariate Distance-Based Matrix Regression (MDMR) results: panels above illustrate the MDMR statistical z-score map indicating brain regions whose interindividual variation in connectivity is significantly associated with A-DMC scores (GRF corrected; $p < .01$). Color bar represents range of z-score values

3 | RESULTS

3.1 | Brain regions associated with individual differences in A-DMC

Figure 1 illustrates the map of significant regions associated with individuals' A-DMC composite scores (summarized in Table 1). A broadly distributed pattern of cortical regions was observed, including brain structures in frontal, parietal, temporal and occipital cortex. Significant associations were observed for regions known to mediate executive functions and language processing (frontal pole and inferior frontal gyrus); visuospatial and attentional processing (lateral occipital cortex and precuneus); emotion and memory (insular cortex, caudate, anterior cingulate gyrus, and parahippocampal gyrus); and sensorimotor processing (precentral and postcentral gyrus).

3.2 | Networks influenced by A-DMC sensitive brain regions

Results from the SEM path analysis are shown in Table 2, which displays the direction and degree of association between network influence of A-DMC sensitive regions on each of the seven ICNs and individual subtests of the A-DMC battery (i.e., resistance to framing, resistance to sunk costs, under/over confidence, consistency in risk perception, recognizing social norms, and applying decision rules). Notably, the ventral attention network predicted individual differences in resistance to framing ($\beta = 0.127$; $p = .012$). Also, significant associations were found between measures of network influence and individual differences in recognizing social norms for the limbic and fronto-parietal networks ($\beta = 0.157$; $p = .006$ and $\beta = 0.154$; $p = .003$, respectively). In addition, we found

that the influence of A-DMC sensitive regions on the limbic network predicted individual differences in performance on the under/over confidence ($\beta = -0.146$; $p = .010$) and recognizing social norms subtests ($\beta = 0.110$; $p = .066$). We found that there was no significant association between A-DMC sensitive regions and three ICNs, namely, the visual, somatomotor, and dorsal attention networks, and individual subtests of the A-DMC battery (range weights: $-.096$ to $.080$). The SEM findings are summarized in Figure 2.

4 | DISCUSSION

This study applied multivariate methods to investigate the neural mechanisms underlying individual differences in decision making competence, examining connections across the entire functional brain connectome, administering a comprehensive and well-validated measure of decision making competence, and studying a large sample of participants ($N = 304$). Our findings lend support for an integrative framework that combines neural representations for (1) executive functions, (2) social factors, and (3) perceptual processes to investigate decision making competence. We briefly review the implications of the MDMR and SEM results in the context of these neural representations.

4.1 | Executive functions

MDMR results revealed that decision making competence was associated with frontopolar regions mediating executive functions. Further evidence for the role of executive functions in decision making is supported by the SEM results linking recognizing social norms with the fronto-parietal network. The fronto-parietal network is known to mediate executive functions, such as goal-directed behavior, inhibitory

TABLE 1 MDMR results

| Voxels | Max | X | Y | Z | Region |
|--------|------|-------|-------|-------|-----------|
| 125 | 2.91 | -2.14 | -60.7 | 60.4 | L. PCUN |
| 97 | 3.24 | 9.96 | -91.8 | -1.96 | R. OCP |
| 78 | 2.85 | -4.77 | -20.6 | 58.9 | L. PRECG |
| 52 | 3.24 | -24.9 | -95.2 | -6.19 | L. OCP |
| 37 | 2.38 | -42.4 | -1.03 | 0.432 | L. INSC |
| 30 | 3.16 | 66.1 | -46.5 | 5.33 | R. MTG |
| 28 | 2.55 | -23.9 | -4 | -25.6 | L. PHG |
| 27 | 2.41 | -11.6 | 11.8 | -9.48 | L. CAUD |
| 26 | 2.6 | -38.6 | -3.69 | 43.4 | L. PRECG |
| 26 | 2.51 | 54 | 25.8 | -1.85 | L. IFG |
| 25 | 2.39 | -6.16 | 45.5 | -3.84 | L. PCNG |
| 23 | 2.6 | -35.2 | -27.9 | 61.6 | L. POSTCG |
| 22 | 2.42 | -40.9 | -68.9 | 18.2 | L. LOCC |
| 21 | 2.34 | 3.14 | 13.4 | 28.4 | R. ACNG |
| 20 | 2.44 | -25 | 46.2 | 19 | L. FP |
| 20 | 3.04 | 7 | 14.2 | -8.2 | R. CAUD |
| 19 | 2.5 | -25.4 | 0.105 | 9.68 | L. PUT |

Abbreviations: ACNG = anterior cingulate gyrus; CAUD = caudate; FP = frontal pole; IFG = inferior frontal gyrus; INSC = insular cortex; L./R. = left/right hemisphere; LOCC = lateral occipital cortex; MTG = middle temporal gyrus; OCP = occipital pole; PCNG = paracingulate gyrus; PCUN = precuneus; PHG = parahippocampal gyrus; POSTCG = postcentral gyrus; PRECG = precentral gyrus; PUT = putamen. Seventeen clustered brain regions were identified using FSL "autoaq" tool from the MDMR output map demonstrating individual differences in functional connectivity that are associated with the A-DMC weighted scores ($p < .01$, cluster corrected using GRF). The columns in Table 1 indicate the number of voxels belonging to each identified cluster, the maximum z-score value in each cluster, the center of mass coordinates (X, Y, Z) in MNI space and region labels.

control, attention, and strategic planning (Cole, Repovs, & Anticevic, 2014). Therefore, the functional coupling between the A-DMC sensitive regions and the fronto-parietal network draws upon inhibitory

control mechanisms, for example, to resist options that are negatively perceived in the social context.

4.2 | Social and emotional factors

We observed significant associations between decision making competence and regions implicated with the limbic system regulating emotion and reward based responses. Notably, the anterior cingulate gyrus, which has been reported to play a central role in reward-based decision making (Assadi, Yucel, & Pantelis, 2009; Rushworth, Behrens, Rudebeck, & Walton, 2007) was found to be significant. Other significant regions included the insular cortex, paracingulate cortex, parahippocampal gyrus, the caudate, and putamen, which have been known to modulate social and emotional components of decision making competence (Kable & Glimcher, 2009; Lee, 2008). SEM results, on the other hand, show positive association between the limbic network and recognizing social norms in decision making. This finding suggests that the limbic network may contribute to behavioral patterns and choices based on subjective states and interoceptive awareness with respect to social norms. Previous studies have indicated that the limbic system is important for decision making, specifically for choices that are influenced by emotional factors (Ernst & Paulus, 2005; Lee, 2008; Marschner, et al., 2005). Interestingly, the limbic network was negatively associated with the under/over confidence A-DMC subtest. The under/over confidence subtest is designed to assess an individual's degree of confidence in their decision. Recent evidence suggests that the ventromedial and rostrolateral prefrontal cortex play a central role in the representation of one's confidence in decision making (De Martino, Fleming, Garrett, & Dolan, 2013). In this study, the observed pattern of reduced functional connectivity in the limbic network and higher connectivity in brain networks mediating executive control may reflect the assessment of subjective confidence based on executive (rather than emotional) mechanisms.

4.3 | Somatosensory and perceptual processes

The MDMR analysis revealed regions within the somatosensory area such as the precentral and postcentral gyrus that are sensitive to

TABLE 2 Direct weights indicating degree and direction of association between network measures of influence of A-DMC-sensitive regions with respect to each ICN and A-DMC subtests

| ICN | A-DMC subtests | | | | | |
|-------------------|-----------------------|--------------------------|-----------------------|-------------------------|--------------------------------|--------------------------|
| | Resistance to framing | Recognizing social norms | Under/over confidence | Applying decision rules | Consistency in risk perception | Resistance to sunk costs |
| Visual | -0.063 | -0.006 | -0.014 | 0.005 | 0.005 | -0.009 |
| Somatomotor | 0.080 | 0.077 | -0.058 | 0.003 | 0.052 | 0.053 |
| Dorsal attention | -0.014 | 0.067 | -0.030 | -0.097 | 0.020 | 0.021 |
| Ventral attention | 0.127* | 0.080° | -0.068 | 0.026 | -0.007 | 0.032 |
| Limbic | 0.052 | 0.156* | -0.146* | 0.026 | 0.110 | 0.026 |
| Fronto-parietal | 0.066 | 0.154* | -0.044 | 0.075 | 0.049 | 0.031 |
| Default mode | 0.051 | 0.108 | -0.027 | 0.115 | 0.089 | 0.048 |

Statistical significance: * $p < .05$.

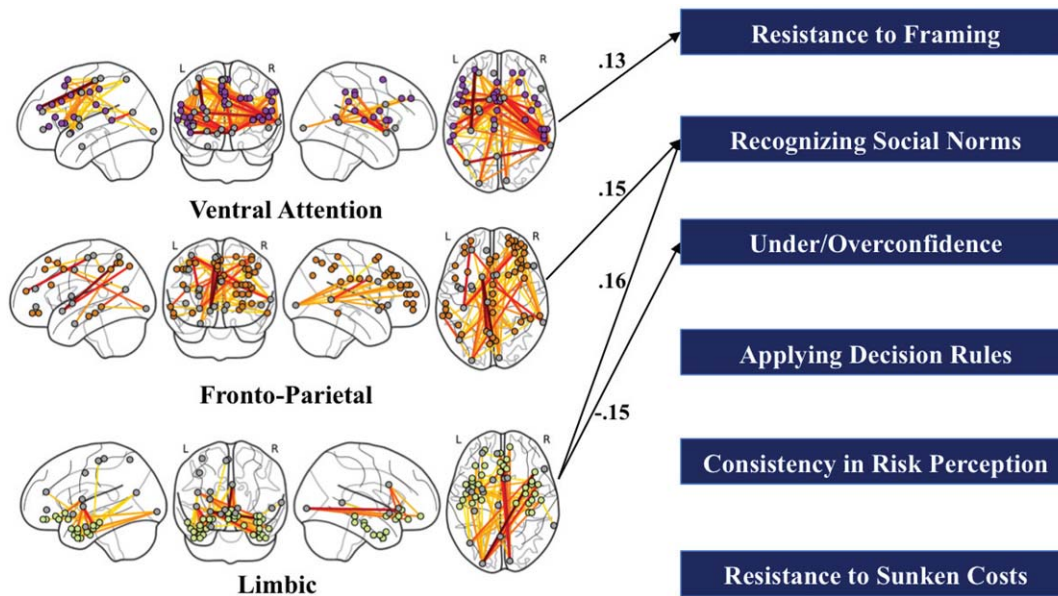


FIGURE 2 SEM results: significant (solid line) associations between measures of network influence of A-DMC sensitive regions (grey nodes) with respect to ICNs (purple, orange, and yellow nodes) and A-DMC subtests

individual differences in decision making competence. These regions are responsible for initiating and controlling bodily and physiological states, and therefore may contribute to decision making via the simulation of choice outcomes based on motor efference copy (Sperduti, Delaveau, Fossati, & Nadel, 2011). In addition, individual differences in decision making competence were associated with regions within the parietal lobe, including the precuneus. Evidence from a recent study indicates that the precuneus has differential connectivity within the default mode network across individuals' lifespan (Yang, et al., 2014) and have specialized roles in self-related cognition and awareness (Philippi, et al., 2012; Whitfield-Gabrieli, et al., 2011). These specific attributes of the precuneus suggest that it may be intimately linked with decision making outcomes that depend on over/under-confidence or other metacognitive abilities. SEM results also support that decision making competence is closely tied to neural mechanisms in perception. Notably, we observed that the ventral attention network was positively associated with resistance to framing, which assesses an individual's ability to ignore irrelevant variations in the decision problem. The ventral attention network is known to orient cognitive resources to salient stimuli in the environment and suppress nonrelevant signals (Fox, Corbetta, Snyder, Vincent, & Raichle, 2006; Seeley, et al., 2007). Hence, functional interaction between the ventral attention network and the A-DMC sensitive regions could modulate perceptual processes that assist in evaluating framing effects in decision making.

5 | LIMITATIONS

While this work represents one of the largest ($N = 304$) and most comprehensive studies to investigate individual differences in the neural mechanisms of decision making competence, there are several limitations. First, our study is based on an individual difference measure, which maps brain regions associated with variability in A-DMC

composite scores. Future research should examine the extent to which the observed results differ from those derived from standard univariate group based methods. Comparison of these approaches would reveal important neural mechanisms that underlie decision making competence that are common across the sample population and would complement the current findings. Second, our MDMR findings provide converging evidence for brain regions linked to decision making competence based on resting-state fMRI data; further research should test the hypothesis that task-related brain activation and connectivity will engage the same (or a subset) of the networks identified in this resting state analysis. Third, our study maps linear relationships between measures of network influence and A-DMC subtests. Given the complex nature of interactions between different brain regions and networks, the findings may not reflect higher order or nonlinear relationships between distributed brain regions and neural systems that explains individual differences in A-DMC subtests. Thus, future research should further examine higher order and nonlinear relationships to replicate and extend this study. Finally, this study examined individual differences within a large sample of healthy young adults ($N = 304$) and should be investigated in a replication study that employs multiple strategies for statistical validation to assess whether the observed sources of interindividual differences generalize beyond this sample.

6 | CONCLUSION

This study provides a novel lens for understanding the role of the functional brain connectome in complex, real-world behavior—demonstrating that individual differences in functional connectivity contribute to decision making competence. Our findings help to establish the efficacy of a multivariate approach to study the neurobiological foundations of decision making and set the stage for future research investigating how the observed sources of individual differences—

represented within networks for executive, social, and perceptual processes—account for the richness and complexity of human judgment and decision making.

ACKNOWLEDGMENTS

The work was supported by the Office of the Director of National Intelligence (ODNI), Intelligence Advanced Research Projects Activity (IARPA), via Contract 2014-13121700004 to the University of Illinois at Urbana-Champaign (PI: Barbey). The views and conclusions contained herein are those of the authors and should not be interpreted as necessarily representing the official policies or endorsements, either expressed or implied, of the ODNI, IARPA, or the U.S. Government. The U.S. Government is authorized to reproduce and distribute reprints for Governmental purposes notwithstanding any copyright annotation thereon. The authors would like to thank the team of investigators, fellows, students, and staff that made the Illinois INSIGHT study possible (for further details, please see: <http://insight.beckman.illinois.edu/team.html>).

ORCID

Tanveer Talukdar  <http://orcid.org/0000-0002-0109-6636>

REFERENCES

- Arkes, H. R., & Blumer, C. (1985). The psychology of sunk cost. *Organizational Behavior and Human Decision Processes*, 35(1), 124–140.
- Assadi, S. M., Yucel, M., & Pantelis, C. (2009). Dopamine modulates neural networks involved in effort-based decision-making. *Neuroscience & Biobehavioral Reviews*, 33(3), 383–393.
- Auerbach, E. J., Xu, J., Yacoub, E., Moeller, S., & Ugurbil, K. (2013). Multi-band accelerated spin-echo echo planar imaging with reduced peak RF power using time-shifted RF pulses. *Magnetic Resonance in Medicine*, 69(5), 1261–1267.
- Bechara, A., Damasio, H., & Damasio, A. R. (2000a). Emotion, decision making and the orbitofrontal cortex. *Cerebral Cortex (New York, N.Y. : 1991)*, 10(3), 295–307.
- Bechara, A., Tranel, D., & Damasio, H. (2000b). Characterization of the decision-making deficit of patients with ventromedial prefrontal cortex lesions. *Brain*, 123(Pt 11), 2189–2202.
- Bruine de Bruin, W., Parker, A. M., & Fischhoff, B. (2007). Individual differences in adult decision-making competence. *Journal of Personality and Social Psychology*, 92(5), 938.
- Cole, M. W., Repovs, G., & Anticevic, A. (2014). The frontoparietal control system: A central role in mental health. *The Neuroscientist*, 20(6), 652–664.
- Craddock, R. C., James, G. A., Holtzheimer, P. E., Hu, X. P., & Mayberg, H. S. (2012). A whole brain fMRI atlas generated via spatially constrained spectral clustering. *Human Brain Mapping*, 33(8), 1914–1928.
- De Martino, B., Fleming, S. M., Garrett, N., & Dolan, R. J. (2013). Confidence in value-based choice. *Nature Neuroscience*, 16(1), 105–110.
- Ernst, M., & Paulus, M. P. (2005). Neurobiology of decision making: A selective review from a neurocognitive and clinical perspective. *Biological Psychiatry*, 58(8), 597–604.
- Fellows, L. K., & Farah, M. J. (2004). Different underlying impairments in decision-making following ventromedial and dorsolateral frontal lobe damage in humans. *Cerebral Cortex (New York, N.Y. : 1991)*, 15(1), 58–63.
- Fox, M. D., Corbetta, M., Snyder, A. Z., Vincent, J. L., & Raichle, M. E. (2006). Spontaneous neuronal activity distinguishes human dorsal and ventral attention systems. *Proceedings of the National Academy of Sciences of the United States of America*, 103(26), 10046–10051.
- Fox, M. D., Zhang, D., Snyder, A. Z., & Raichle, M. E. (2009). The global signal and observed anticorrelated resting state brain networks. *Journal of Neurophysiology*, 101(6), 3270–3283.
- Glascher, J., Adolphs, R., Damasio, H., Bechara, A., Rudrauf, D., Calamia, M., ... Tranel, D. (2012). Lesion mapping of cognitive control and value-based decision making in the prefrontal cortex. *Proceedings of the National Academy of Sciences of the United States of America*, 109(36), 14681–14686.
- Hornak, J., Bramham, J., Rolls, E. T., Morris, R. G., O'Doherty, J., Bullock, P. R., & Polkey, C. E. (2003). Changes in emotion after circumscribed surgical lesions of the orbitofrontal and cingulate cortices. *Brain*, 126(7), 1691–1712.
- Jacobs, J. E., Greenwald, J. P., & Osgood, D. W. (1995). Developmental differences in baserate estimates of social behaviors and attitudes. *Social Development*, 4(2), 165–181.
- Jenkinson, M., Beckmann, C. F., Behrens, T. E. J., Woolrich, M. W., & Smith, S. M. (2012). FSL. *NeuroImage*, 62(2), 782–790.
- Kable, J. W., & Glimcher, P. W. (2009). The neurobiology of decision: Consensus and controversy. *Neuron*, 63(6), 733–745.
- Kiani, R., & Shadlen, M. N. (2009). Representation of confidence associated with a decision by neurons in the parietal cortex. *Science (New York, N.Y.)*, 324(5928), 759–764.
- Krain, A. L., Wilson, A. M., Arbuckle, R., Castellanos, F. X., & Milham, M. P. (2006). Distinct neural mechanisms of risk and ambiguity: A meta-analysis of decision-making. *NeuroImage*, 32(1), 477–484.
- Laird, A. R., Fox, P. M., Eickhoff, S. B., Turner, J. A., Ray, K. L., McKay, D. R., ... Fox, P. T. (2011). Behavioral interpretations of intrinsic connectivity networks. *Journal of Cognitive Neuroscience*, 23(12), 4022–4037.
- Lee, D. (2008). Game theory and neural basis of social decision making. *Nature Neuroscience*, 11(4), 404–409.
- Li, K., Guo, L., Nie, J., Li, G., & Liu, T. (2009). Review of methods for functional brain connectivity detection using fMRI. *Computerized Medical Imaging and Graphics*, 33(2), 131–139.
- Marschner, A., Mell, T., Wartenburger, I., Villringer, A., Reischies, F. M., & Heekeren, H. R. (2005). Reward-based decision-making and aging. *Brain Research Bulletin*, 67(5), 382–390.
- Murphy, K., Birn, R. M., Handwerker, D. A., Jones, T. B., & Bandettini, P. A. (2009). The impact of global signal regression on resting state correlations: Are anti-correlated networks introduced? *NeuroImage*, 44(3), 893–905.
- Muthén, L. K., Muthén, B. O. (2007). *Mplus User's Guide (Sixth Edition)*. Los Angeles, CA: Muthén & Muthén.
- Payne, J. W., Bettman, J. R., & Johnson, E. J. (1993). *The adaptive decision maker*. Cambridge University Press.
- Philippi, C. L., Feinstein, J. S., Khalsa, S. S., Damasio, A., Tranel, D., Landini, G., ... Rudrauf, D. (2012). Preserved self-awareness following extensive bilateral brain damage to the insula, anterior cingulate, and medial prefrontal cortices. *PLoS One*, 7(8), e38413.
- Power, J. D., Barnes, K. A., Snyder, A. Z., Schlaggar, B. L., & Petersen, S. E. (2012). Spurious but systematic correlations in functional connectivity MRI networks arise from subject motion. *NeuroImage*, 59(3), 2142–2154.
- Rubinov, M., & Sporns, O. (2010). Complex network measures of brain connectivity: Uses and interpretations. *NeuroImage*, 52(3), 1059–1069.

- Rudorf, S., & Hare, T. A. (2014). Interactions between dorsolateral and ventromedial prefrontal cortex underlie context-dependent stimulus valuation in goal-directed choice. *Journal of Neuroscience*, 34(48), 15988–15996.
- Rushworth, M. F., Behrens, T. E., Rudebeck, P. H., & Walton, M. E. (2007). Contrasting roles for cingulate and orbitofrontal cortex in decisions and social behaviour. *Trends in Cognitive Sciences*, 11(4), 168–176.
- Satterthwaite, T. D., Elliott, M. A., Gerraty, R. T., Ruparel, K., Loughhead, J., Calkins, M. E., ... Wolf, D. H. (2013). An improved framework for confound regression and filtering for control of motion artifact in the preprocessing of resting-state functional connectivity data. *NeuroImage*, 64, 240–256.
- Seeley, W. W., Menon, V., Schatzberg, A. F., Keller, J., Glover, G. H., Kenna, H., ... Greicius, M. D. (2007). Dissociable intrinsic connectivity networks for salience processing and executive control. *Journal of Neuroscience*, 27(9), 2349–2356.
- Shadlen, M. N., & Newsome, W. T. (2001). Neural basis of a perceptual decision in the parietal cortex (area LIP) of the rhesus monkey. *Journal of Neurophysiology*, 86(4), 1916–1936.
- Shehzad, Z., Kelly, C., Reiss, P. T., Cameron Craddock, R., Emerson, J. W., McMahon, K., ... Milham, M. P. (2014). A multivariate distance-based analytic framework for connectome-wide association studies. *NeuroImage*, 93, 74–94.
- Smith, S. M. (2002). Fast robust automated brain extraction. *Human Brain Mapping*, 17(3), 143–155.
- Sperduti, M., Delaveau, P., Fossati, P., & Nadel, J. (2011). Different brain structures related to self- and external-agency attribution: A brief review and meta-analysis. *Brain Structure and Function*, 216(2), 151–157.
- Stuss, D. T., Levine, B., Alexander, M. P., Hong, J., Palumbo, C., Hamer, L., ... Izukawa, D. (2000). Wisconsin Card Sorting Test performance in patients with focal frontal and posterior brain damage: Effects of lesion location and test structure on separable cognitive processes. *Neuropsychologia*, 38(4), 388–402.
- Talukdar, T., Nikolaidis, A., Zwillig, C. E., Paul, E. J., Hillman, C. H., Cohen, N. J., ... Barbey, A. K. (2017). Aerobic fitness explains individual differences in the functional brain connectome of healthy young adults. *Cerebral Cortex*, 1–10.
- Tversky, A., & Kahneman, D. (1981). Evidential impact of base rates.
- Van Dijk, K. R. A., Hedden, T., Venkataraman, A., Evans, K. C., Lazar, S. W., & Buckner, R. L. (2010). Intrinsic functional connectivity as a tool for human connectomics: Theory, properties, and optimization. *Journal of Neurophysiology*, 103(1), 297–321.
- Whitfield-Gabrieli, S., Moran, J. M., Nieto-Castanon, A., Triantafyllou, C., Saxe, R., & Gabrieli, J. D. (2011). Associations and dissociations between default and self-reference networks in the human brain. *NeuroImage*, 55(1), 225–232.
- Yang, T., & Shadlen, M. N. (2007). Probabilistic reasoning by neurons. *Nature*, 447(7148), 1075–1082.
- Yang, Z., Chang, C., Xu, T., Jiang, L., Handwerker, D. A., Castellanos, F. X., ... Zuo, X. N. (2014). Connectivity trajectory across lifespan differentiates the precuneus from the default network. *NeuroImage*, 89, 45–56.
- Yeo, B. T., Krienen, F. M., Sepulcre, J., Sabuncu, M. R., Lashkari, D., Hol-linshead, M., ... Buckner, R. L. (2011). The organization of the human cerebral cortex estimated by intrinsic functional connectivity. *Journal of Neurophysiology*, 106(3), 1125–1165.
- Zhang, Y., Brady, M., & Smith, S. (2001). Segmentation of brain MR images through a hidden Markov random field model and the expectation-maximization algorithm. *IEEE Transactions on Medical Imaging*, 20(1), 45–57.

How to cite this article: Talukdar T, Román FJ, Operskalski JT, Zwillig CE, Barbey AK. Individual differences in decision making competence revealed by multivariate fMRI. *Hum Brain Mapp*. 2018;00:1–9. <https://doi.org/10.1002/hbm.24032>